Unique growth mode observed in a Pb thin film on the 3-fold surface of an *i*–Ag–In–Yb quasicrystal

Sam Coates, Stuart Thorn, Ronan McGrath, and Hem Raj Sharma
Surface Science Research Centre and Department of Physics, University of Liverpool, Liverpool, L69 3BX, UK

An Pang Tsai
Institute of Multidisciplinary Research for Advanced Materials (IMRAM), Tohoku University, 2–1–1 Katahira, Aoba–ku, Sendai 980–8577, Japan

Novel epitaxial quasicrystalline films can be grown using the surfaces of inter–metallic quasicrystals as templates. Here, we present a study of Pb adsorption on the 3–fold *i*–Ag–In–Yb surface, where Pb grows in a manner contrasting with conventional thin film growth modes. Pb atoms are found to adsorb at sites over a range of heights, which are explained by bulk atomic positions left vacant by surface truncation, producing three–dimensional, isolated quasicrystalline Pb structures. This finding is contrasted with the growth of Pb on the more commonly used 5–fold surface of the same quasicrystal, where smooth epitaxial layers result. We suggest that this unique structure originates due to the lower atomic density of the 3–fold surface, compared to the 5–fold surface. Similar atomic density can be found in lower symmetry planes of periodic systems, but these planes are often unstable and become facetted. This stable low–density quasicrystalline substrate provides a facile route to achieve this type of templated growth.

I. INTRODUCTION

Quasicrystals are materials which exhibit long–range order, yet are aperiodic [1]. As a result, they can exhibit intriguing geometric arrangements with unusual rotational symmetries which can be mapped using aperiodic tilings (e.g. the Penrose tiling [2]). In previous work, the surfaces of inter–metallic quasicrystals have been utilised to produce epitaxial networks with exotic structures, where atoms and molecules occupy specific adsorption sites, creating highly ordered single constituent quasicrystalline structures which have been 'templated' by the surface structure [3–15].

A notable example is the deposition of Pb onto the 5–fold surface of the icosahedral (*i*)–Ag–In–Yb quasicrystal, which possesses 2–, 3–, and 5–fold symmetry axes. The bulk structure of *i*–Ag–In–Yb is modelled using *i*–Cd–Yb Tsai–type clusters, a hierarchical system of polyhedral 'shells' which are decorated with either Cd or Yb (with Ag/In replacing Cd equally) [16]. Figure 1(a) shows the polyhedra (tetrahedron, dodecahedron, icosahedron, icosidodecahedron, and rhombic triacontahedron) which we will refer to as 1^{st}–5^{th} shells respectively. These clusters are distributed aperiodically throughout the bulk with orientations defined by the high symmetry directions. They are joined by 'glue' units – interstitial polyhedra which are separate from the Tsai–type cluster [16].

When Pb is deposited onto the 5–fold *i*–Ag–In–Yb surface, it is found to grow in a quasicrystalline layer–by–layer fashion, with the adsorption sites of each layer mirroring the structure of specific planes of atoms from the bulk model [17]. Figure 1(b) illustrates this. Here, a truncated Tsai–type cluster is shown with the 4^{th} shell in blue. The cluster centre is marked with a golden atom. A horizontal arrow indicates the truncation i.e. the surface. Shown above this truncation are positions of atoms of the 4^{th} shell (shown as hollow circles), if cluster growth were to be continued above the surface. At the 5–fold *i*–Ag–In–Yb surface, Pb is found to sit at certain positions and heights which can be explained by occupation of such bulk-like planes [17]. The same has been found true for other elements, for example Bi [18].

In this work, we show that this type of adsorption behaviour is not specific to the 5–fold termination of the *i*–Ag–In–Yb system. By dosing Pb onto the 3–fold *i*–Ag–In–Yb surface we observe the same general growth method; however, the resultant structure is different in nature. Here, instead of a layer–by–layer system, we observe isolated Pb structures which grow perpendicular to the surface. We link this behaviour to the relative change in density of available adsorption sites between the 3–fold and 5–fold surfaces.

II. METHODS

The 3–fold surface of an *i*–Ag–In–Yb QC was polished with successively finer grades of diamond paste (6–0.25 μm) before washing in methanol. After insertion into an ultra–high vacuum chamber, the surface was cleaned with sputter–anneal cycles (30 minute Ar^+ sputter, 2 hour anneal at 700 K). Substrate cleanliness was monitored with low energy electron diffraction (LEED) and STM.

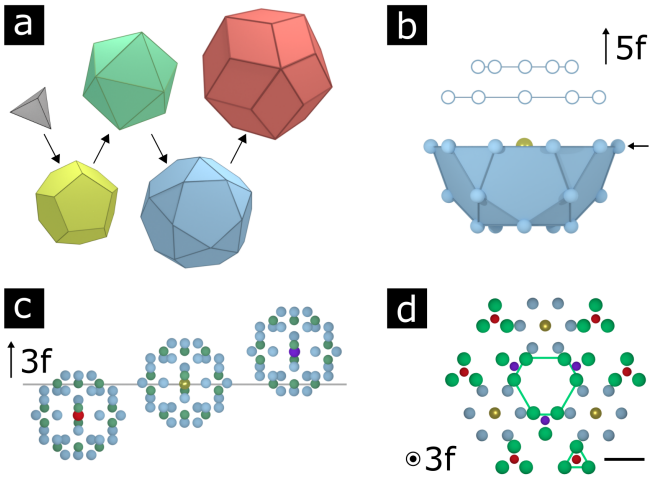

FIG. 1: (a) The hierarchical *i*–Cd–Yb cluster model. A Cd tetrahedron (grey), Cd dodecahedron (yellow), Yb icosahedron (green), Cd icosidodecahedron (blue), and Cd rhombic triacontahedron (red), are arranged concentrically to form the Tsai–type cluster. Arrows indicate hierarchy. (b) Side view of the 4$^{\text{th}}$ shell of a truncated cluster, oriented along its 5–fold direction. The 5–fold surface is marked with an arrow. The cluster centre is shown as a golden atom. Also shown are planes of atoms from the 4$^{\text{th}}$ shell, if the structure was continued 'above' the surface. (c) Side view of how truncated clusters contribute to the 3-fold surface. Horizontal scale is arbitrary. (d) Arrangement of truncated bulk clusters as observed on the surface. A distorted hexagon and a triangle are marked to compare to STM images. Scale bar is 1 nm.

Pb was evaporated at a constant flux of 120 nA onto the surface using a Focus EFM 3 evaporator.

III. RESULTS

The clean 3–fold surface of the *i*–Ag–In–Yb quasicrystal has previously been explored by STM [19]. When observed with non–atomic resolution, the surface appears to be populated by protrusions which form a quasicrystalline network of bright flower–like triangles and so–called 'distorted' hexagons. Atomic resolution is achieved through positive bias (reported as under +1.5 V), where these larger protrusions are revealed to consist of sets of individual atoms. Figure 2(a) shows an example of the previously identified flower/distorted hexagon structure, with both motifs labelled. Vacancies are also highlighted by white circles. Figure 1(d) shows the equivalent structure in the model, with a distorted hexagon, marked in green, formed by Yb atoms. A small triangle is also highlighted, which forms one of the vertices of the flower motifs. In both non–atomic and atomic resolution cases, only Yb atoms are observed [19].

Due to the low atomic density of the surface and Yb atom bias, the substrate appears rough using STM so that clearly resolving Pb atoms and their subsequent adsorption sites is difficult at low to medium coverages. The approach we take is to deposit Pb for a length of time similar to that used to obtain sub–monolayer coverage on the 5–fold surface [17]. Then, assuming that the 3–fold surface has a similar sticking coefficient to the 5–fold, we can compare the height and morphology of the Pb–dosed surface to the clean 3–fold surface.

Figure 2(b) shows an STM image of the surface after depositing Pb for 10 minutes, which would produce an approximate coverage of ∼0.5 monolayers on the 5–fold surface. Here, Pb protrusions form a morphologically rough quasicrystalline network, with many triangular features observed. The size of the individual spots which build the vertices of the triangular features suggests that multiple Pb atoms are contributing to each protrusion – Figures 2(a) and (b) are the same scale, yet the protrusions in Figure 2(b) appear larger than those in Figure 2(a). Two triangular Pb motifs, labelled as 1 and 2, have been highlighted in Figure 2(b), and the edge lengths are noted in Table I. Motifs rotated by 60° which share these edge lengths are marked by dotted lines. The quasicrystalline ordering of the Pb is evidenced by the inset FFT, which was taken after isolating the Pb atoms in the image (i.e. filtering out the substrate contribution). High intensity spots are scaled by τ, a hallmark of aperiodic order in quasicrystals.

To clearly distinguish the Pb atoms from the rough substrate, height histograms have been calculated from both Figures 2(a) and 2(b). Figure 2(c) shows the histogram taken from the substrate. The main peak is broad, a reflection of the surface roughness, with the presence of vacancy defects and partial fragments of an incomplete terrace. The main peak also shows a slight asymmetry towards higher z values, which is indicative of the 'flower' arrangements occasionally appearing brighter. Figure 2(d) shows the histogram from the Pb–dosed surface in Figure 2(b). It has a different distribution to that of the substrate histogram, with a sharp peak bearing a shoulder to its left, at lower z. We attribute the higher peak to the Pb atoms, with the shoulder on the left originating from the surface. The small number of counts at higher z values are due to the growth of Pb atoms at a second height, discussed later.

To highlight the difference between the two histograms, a composite is shown in Figure 2(e). As the separate histograms show the absolute distribution of heights within each image – the definition of z=0 is dependent on the individual scan – this composite has been shifted so that the substrate peaks overlap, and scaled to allow for a direct comparison. The difference in shape and heights between the two plots clearly differentiates the Pb signal

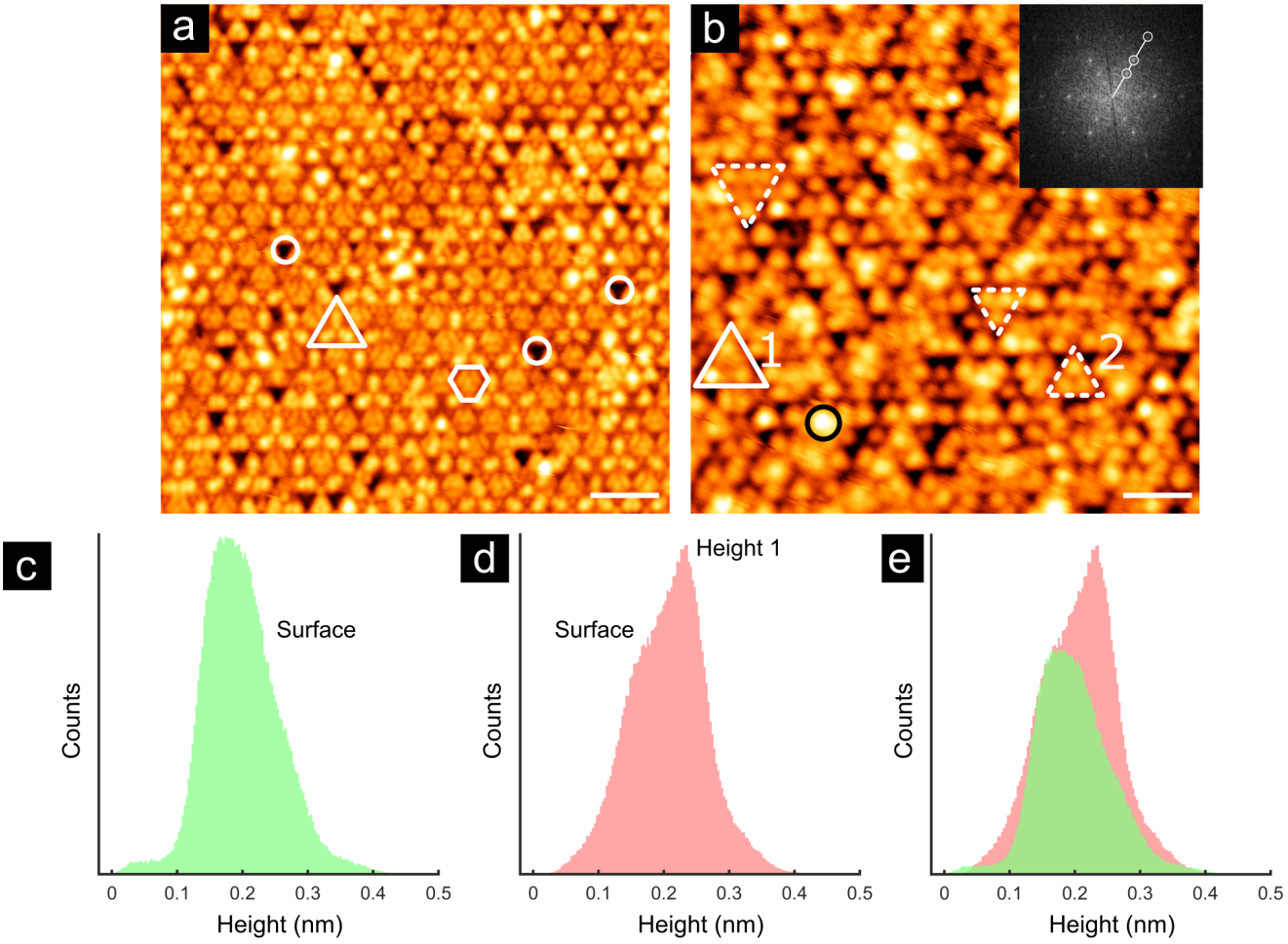

FIG. 2: (a) STM image of the clean substrate. Scale bar is 6 nm. Highlighted in white are triangles and distorted hexagons. (b) STM image of the surface after Pb dosing for 10 minutes. Scale bar is 6 nm. Highlighted in white and numbered 1 and 2 are two triangular motifs of different edge lengths. The dashed triangles shown have an opposite orientation to motif 1 and 2. The feature marked by a black circle is the start of growth of Pb at the next height. Inset is a Fast Fourier transform (FFT) of the STM image, showing τ–scaled maxima. (c, d) Height histograms taken from (a, b). Labelled in (d) are the contributions from Pb atoms and the surface. (e) A composite of (c) and (d), comparing the distribution of the heights in (a) and (b).

from the substrate.

Figures 3(a–c) shows the substrate after increasing Pb deposition time (15–120 minutes). As the dose time progresses, Pb atoms form a porous, quasicrystalline network of isolated triangular structures at four distinct heights. The quasicrystallinity of the Pb overlayer is shown by an FFT inset in Figure 3(c), considering only atoms at the fourth height. Various motifs are numbered and labelled, and the edge lengths are noted in Table I.

Histograms taken from Figures 3(a) and (c) are shown in Figures 3(d) and (e) respectively. The evolution of the height distribution with respect to coverage can be seen in Figure 3(d). As the surface becomes gradually covered with Pb, the prominence of the substrate shoulder signal is diminished, as the height 2 peak increases in size and sharpness. Large vacancies in the substrate are still observed by STM however, as is apparent from the tail at low z. Figure 3(e) shows the Pb heights at the maximum observed coverage. Here, three peaks are discernible, with the substrate now completely covered by the first height of Pb – evident by the disappearance of the vacancy 'tail' at low z. The prominence of the height 2 peak is also reduced, which indicates that Pb at heights 3 or 4 (or both) are adsorbing directly on top of these atoms. Pb atoms at larger z values than height 4 are also observed, as shown by the small number of counts in Figure 3(e). At much larger dose times ($\sim$ 180 minutes), these atoms begin to form periodic structures.

To compare the overall system of Pb heights, Figure 3(f) shows a composite of the histograms from Figures 2(d) and 3(d–e). Each histogram is coloured as before, with a key showing which heights are represented by each

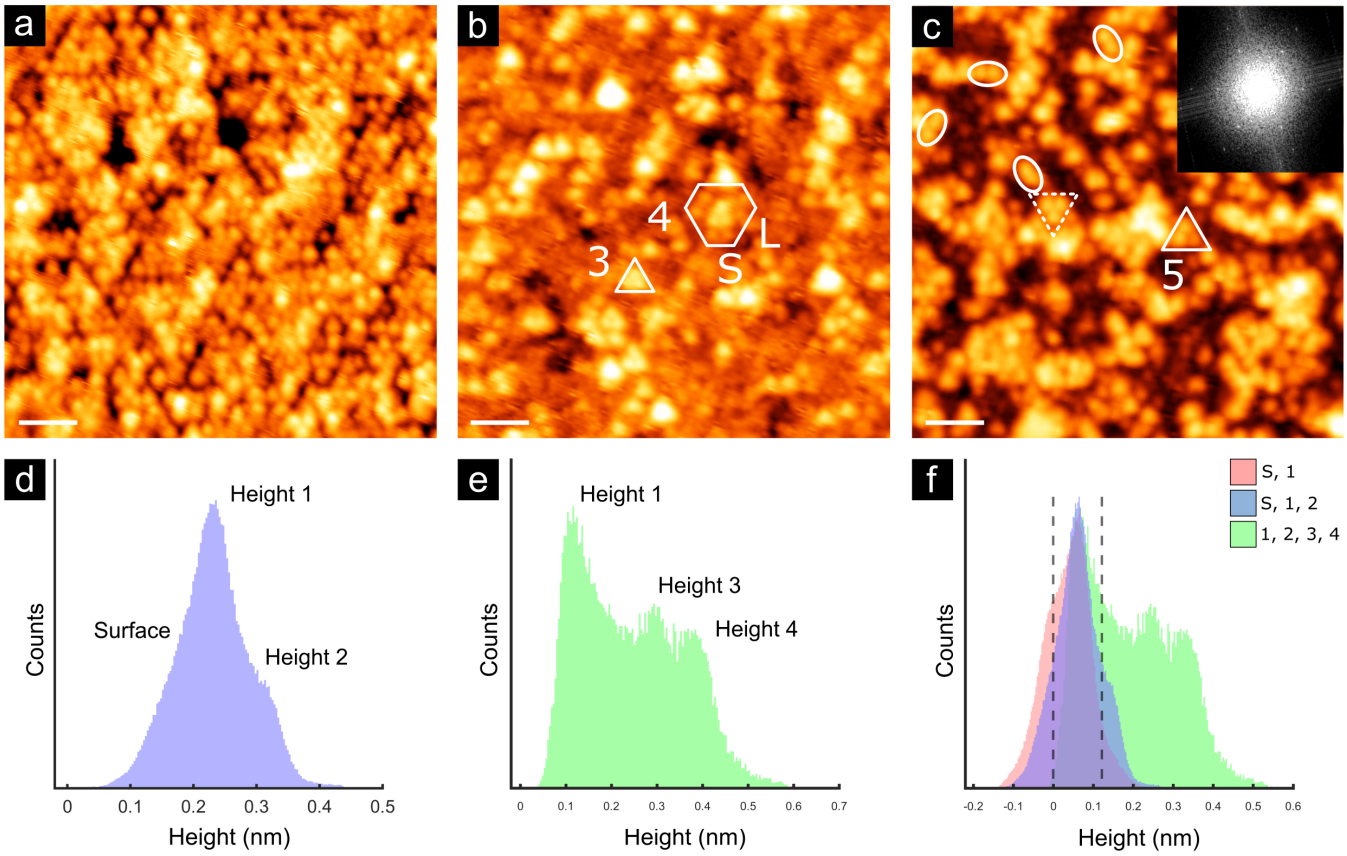

FIG. 3: (a) STM image of the surface after Pb dosing for 15 minutes. Scale bar is 6 nm. (b) STM image of the surface after Pb dosing for 30 minutes. Marked in white is a triangle labelled 3 and a distorted hexagon (4), with edge lengths S and L, listed in Table (I). Scale bar is 6 nm. (c) STM image of the surface after Pb dosing for 120 minutes. Motif 5 is marked by a white triangle – the dashed triangle shown has an opposite orientation. Pb-dimers of the same edge-length as motif 5 are also marked by ovals. Inset is a τ–scaled FFT, taken considering only height 4 atoms. Scale bar is 4 nm. (d–e) Histograms from (a,c). (f) A composite of histograms from (d,e), and Figure 2(d).

chart (S = substrate). Here, the substrate shoulder from the low coverage data has been used as an initial calibration point for comparing Figure 3(d), highlighted with a dashed line at 0 nm. Subsequently, the first height is used as a reference point. The overlap of height 2 in Figure 3(d,e) is shown by the second dashed line, at ~ 0.11 nm. The comparison of the histograms shows the extent to which the overall height distribution is broadened by the additional Pb atoms. Likewise, the defined peaks of the third and fourth heights infer that the Pb produces a network of isolated structures on top of the first layer.

IV. DISCUSSION

A. Adsorption sites of each layer

The distinctive heights of the Pb atoms above the substrate can be recognized from the histograms. Following the methodology in [17], we can compare these values to the heights of planes above the surface in the Cd–Yb model. If a model plane with a similar height for each set of Pb is found, we then compare motifs from these planes to the features formed by the Pb atoms. If a 'match' is found, we attribute the adsorption sites of each height to positions explained by these planes. Figure 4(a) shows the heights and densities of the model planes above the surface, colour–coded to represent and match the shells of the Cd–Yb clusters (Figure 1) which form each plane. Each height is marked, with the corresponding model shell also labelled.

Pb atoms at height 1 can be explained by a plane consisting of atoms from the 5^{th} shells (red) of surface–centred clusters. Its morphology is shown in Figure 4(b), where collections of closely separated Pb atoms form triangular motifs. These dense groups may be the cause of the enlarged protrusions observed in Figure 2(b). Motifs with edge lengths equal to those measured in Figure 2(b) are highlighted, and motif 1 has been enlarged and compared to the data in Figure 4(e).

The adsorption positions of height 2 Pb atoms are diffi-

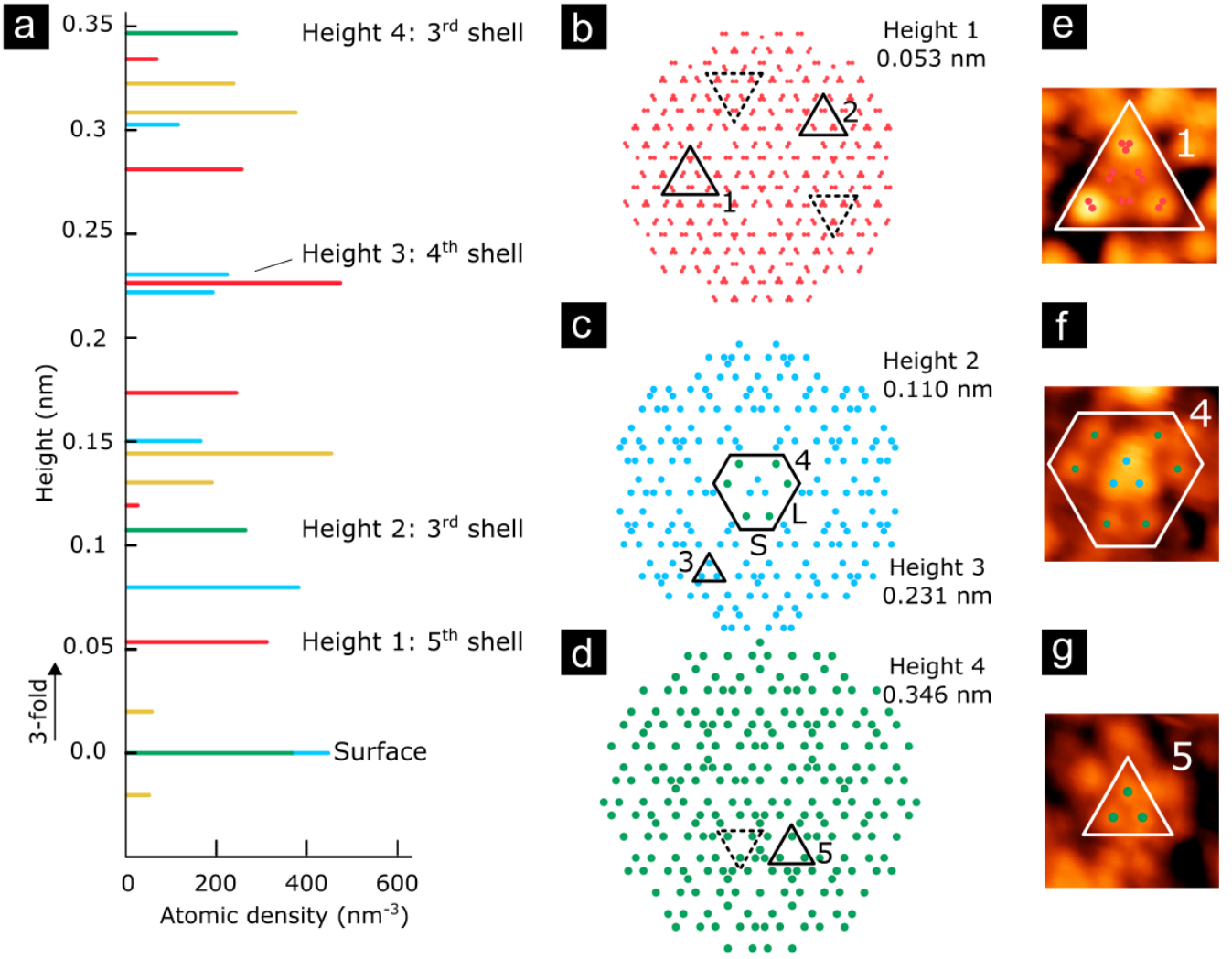

FIG. 4: (a) Distribution of height and density of atoms of *i*-Cd–Yb along the 3–fold direction. Labelled are shells of the bulk clusters which correspond to the observed Pb heights as indicated. The surface plane is also indicated. Color scheme is same as in Figure 1. (b–d) In-plane atomic structure at indicated heights. Marked in each are similar motifs from Figures 2(b), 3(b,c). The heights of the planes are shown above each. Only selected atoms at height 2 are shown for clarity in comparison with STM. (e–g) Selected STM motifs from heights (b–d), respectively.

cult to analyse independently, as these atoms are covered by height 3 atoms quickly. However, we can resolve the third height, then use limited examples of comparative geometry between the second and third heights to find the plane which explains the height 2 Pb atoms. Height 3 Pb atoms largely form only one motif, a small triangle with only one orientation (motif 3). Combining the height of the atoms with this observation leads to the assignment of a plane of 4^{th} shell (blue) atoms originating from surface–centred clusters, shown in Figure 4(c). Now, motif 4, shown in Figure 4(f), is a motif 3 triangle surrounded by 6 atoms at height 2 which create a distorted hexagon. This particular triangle–in–hexagon formation is only observed by STM between these two heights, and likewise only one plane can be used to explain the positions of the height 2 atoms in this structure. Labelled in Figure 4(a), this height is explained by the 3^{rd} shell (green, Yb) of surface–centred clusters. Figure 4(c) shows the superposition of heights 2 and 3 at this formation. The adsorption sites of the final Pb atoms can be explained by 3^{rd} shell (green, Yb) positions of off–surface–centred clusters, labelled in Figure 4(a) and shown in Figure 4(d). As with heights 2 and 3, examples can be found of comparative geometry between heights 3 and 4 which match those seen in the model. In Table I, we collect all of the experimental motif edge lengths and their counterparts identified in the model for comparison.

Height	Height_{STM} (nm)	Height_{model} (nm)
1	0.06 ± 0.01	0.053
2	0.11 ± 0.01	0.110
3	0.23 ± 0.01	0.231
4	0.35 ± 0.02	0.346

Motif	Edge_{STM} (nm)	Edge_{model} (nm)
1	2.6 ± 0.1	2.54
2	1.5 ± 0.1	1.42
3	0.91 ± 0.05	1.04
4(S)	1.47 ± 0.05	1.57
4(L)	2.4 ± 0.1	2.54
5	1.62 ± 0.07	1.57

TABLE I: The heights and edge lengths of motifs of Pb observed in Figures 3(b–d), compared to their model plane counterparts in Figures 4(b–d). Heights are measured with respect to the surface.

	Intra–plane distance (nm)		
Height	NN_1	NN_2	Average
1	0.30*	0.97	0.63
2	0.60	0.97	0.78
3	0.52	1.04	0.78
4	0.60	0.97	0.78

Inter–plane distance (nm)	
Height	NN
S–1	0.32
S–2	0.34
1–2	0.34
1–3	0.32
1–4	0.34
2–3	0.60
3–4	0.32

TABLE II: Top: Intra–layer distances of the model planes. NN_i refers to distances which are observed with equal regularity. The asterisked value shows a nearest neighbour distance close to crystalline Pb. Bottom: Inter–layer distances which are close to crystalline Pb.

B. Stability of quasicrystalline Pb

Pb adsorption sites on the 3–fold *i*–Ag–In–Yb surface can be explained by 'vacant' *i*–Cd–Yb planes in the same way as was found for the 5–fold surface. However, the actual growth mode differs here – rather than a layer–by–layer type, Pb favours growth directly perpendicular to the surface. One explanation is that this is due to the relative change in density of available adsorption sites between these two surfaces.

The major difference (aside from rotational symmetry) between the 3– and 5–fold orientations of *i*–Ag–In–Yb is atomic density within planes perpendicular to these directions. The average number of atoms per plane for the 3–fold direction is 2.6 atoms per nm^2, and, for the 5–fold, 4.6 atoms per nm^2. Likewise, the density of planes in a 1 nm slab in z is 54 planes per nm for the 3–fold direction and 38 planes per nm for the 5–fold direction. In other words, the 3–fold orientation has less atoms per plane, but more planes per nm in z compared to the 5–fold. The implication is that there are a reduced number of available adsorption sites in the 3–fold x–y plane compared to the 5–fold direction. Therefore, once these sites are filled, Pb will occupy preferential sites available in the z-direction.

This observation is strengthened when analysing the nearest neighbour distances between Pb atoms within this growth scheme. The stability and growth mode of Pb on the 5–fold *i*–Ag–In–Yb surface was stabilised by the reduction of nearest neighbour distances [17]. In this case, values close to, or less than, the nearest neighbour value in crystalline (fcc) Pb (0.32 nm) were considered as important in stabilising the film, verified by Density Functional Theory calculations. Employing a similar argument here, Table II shows the nearest neighbour values taken from the 3–fold planes in Figure 4(b–d) for intra–plane (i.e. separations of atoms belonging to the same plane) and inter–plane (separations between different planes) distances. Here, (S–1) refers to the distance measured between a substrate atom and a height 1 atom, etc.

In the intra–plane case, two distances are measured for each model plane, as the nearest neighbour distance can vary on an atom–by–atom basis. The average value for each plane shows that intra–plane nearest neighbour distances are much larger than the bond length for crystalline Pb. However, the values for the inter–plane distances are identical, or close to, the nearest neighbour distance for crystalline Pb (with the exception of heights 2–3). Thus, we hypothesize that to maximise the film's stability, positions in z are prioritized over in–plane growth and, in particular, the height 1 atoms are important for stabilizing the larger height atoms (3 and 4).

To illustrate this argument, Figure 5 shows a truncated Tsai–type cluster which is decorated with coloured atoms. This schematic shows how a single Tsai–cluster can be 'capped' by the four heights of Pb atoms. The colours of the truncated polyhedra and Pb atoms correspond to the similarly coloured shells in Figures 1 and 4(a). Surface atoms are coloured grey, and height 4 atoms coloured purple to differentiate them from the height 2 atoms (both have positions modelled by 3^{rd} shells). The inter–plane nearest neighbour distances are labelled in

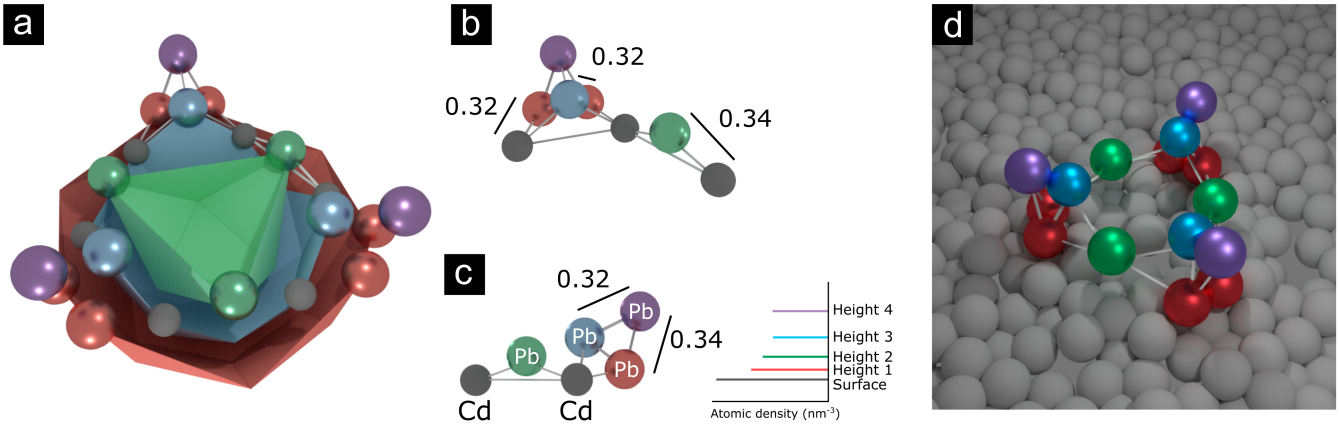

FIG. 5: (a) A Tsai–cluster with 3$^{\text{rd}}$, 4$^{\text{th}}$, and 5$^{\text{th}}$ shells shown as truncated polyhedra. Each shell is decorated with Pb atoms, representing the planes which construct the film. (b) A section of (a) with nearest neighbour values labelled in nm. (c) Side view of (b), with more nearest neighbour values. Adjacent is a planar model with labelled planes for each height. (d) View of (a) on the 3–fold surface, from a different perspective.

Figures 5(b–c), showing how the Pb atoms in the system are stabilised either by the substrate or previous heights, as opposed to atoms of the same height. Finally, Figure 5(d) shows the Pb 'cluster' of Figure 5(a) from a different perspective on a model of the 3–fold surface (grey spheres). According to the Cd–Yb model, these Pb nano–structures would be distributed quasiperiodically over the surface.

V. CONCLUSIONS

We have shown that the growth scheme of Pb observed on the 5–fold *i*–Ag–In–Yb surface also applies to the 3–fold surface. On this substrate, the low in–plane density of the 3–fold surface and the subsequent Pb layers creates a quasicrystalline network with isolated structures forming along *z*. Here, we showcase the usage of a stable, sparse, and uniquely structured quasicrystalline surface which could potentially be used to produce templated nano–structures. The low density of the substrate provides a unique arena for this growth mode – similar atomic sparsity could only be found in a periodic system in a vicinal plane – in which case, the surface becomes unstable and facets. It would be interesting to investigate if adsorption of a stoichiometric blend of elements (e.g. Ag/In/Yb) that constitute the quasicrystal on this surface would indirectly replicate the building block Tsai–type clusters, providing direct evidence of the stability of bulk clusters.

ACKNOWLEDGEMENTS

Partial support for this work from the Engineering and Physical Sciences Research Council (grant number EP/D071828/1) and the European Integrated Centre for the Development of New Metallic Alloys and Compounds is gratefully acknowledged.

[1] D. Shechtman, I. Blech, D. Gratias, and J. W. Cahn, Phys. Rev. Lett. **53**, 1951 (1984).
[2] R. Penrose, The mathematical intelligencer **2**, 32 (1979).
[3] H. R. Sharma, M. Shimoda, and A. P. Tsai, Advances in Physics **56**, 403 (2007).
[4] R. McGrath, J. Ledieu, E. J. Cox, and R. D. Diehl, Journal of Physics: Condensed Matter **14**, R119 (2002).
[5] R. McGrath, J. A. Smerdon, H. R. Sharma, W. Theis, and J. Ledieu, Journal of Physics: Condensed Matter **22**, 084022 (2010).
[6] R. McGrath, H. R. Sharma, J. A. Smerdon, and J. Ledieu, Phil. Trans. of R. Soc. A **370**, 2930 (2012).
[7] S. Coates, J. A. Smerdon, R. McGrath, and H. R. Sharma, Nat. Commun. **9** (2018).
[8] H. R. Sharma, J. A. Smerdon, P. J. Nugent, A. Ribeiro, I. McLeod, V. R. Dhanak, M. Shimoda, A. P. Tsai, and R. McGrath, J. Chem. Phys. **140**, 174710 (2014).
[9] V. Fournée, É. Gaudry, J. Ledieu, M.-C. De Weerd, D. Wu, and T. Lograsso, ACS Nano **8**, 3646 (2014).
[10] J. A. Smerdon, J. Ledieu, J. T. Hoeft, D. E. Reid, L. H. Wearing, R. D. Diehl, T. A. Lograsso, A. R. Ross, and R. McGrath, Philos. Mag. **86**, 841 (2006).
[11] J. A. Smerdon, J. Ledieu, R. McGrath, T. C. Q. Noakes, P. Bailey, M. Draxler, C. F. McConville, T. A. Lograsso, and A. R. Ross, Phys. Rev. B **74**, 035429 (2006).
[12] J. A. Smerdon, L. Leung, J. K. Parle, C. J. Jenks, R. McGrath, V. Fournée, and J. Ledieu, Surf. Sci. **602**, 2496 (2008).

[13] J. A. Smerdon, J. K. Parle, L. H. Wearing, T. A. Lograsso, A. R. Ross, and R. McGrath, Phys. Rev. B **78**, 075407 (2008).

[14] J. A. Smerdon, K. M. Young, M. Lowe, S. S. Hars, T. P. Yadav, D. Hesp, V. R. Dhanak, A. P. Tsai, H. R. Sharma, and R. McGrath, Nano Lett. **14**, 1184 (2014).

[15] K. J. Franke, H. R. Sharma, W. Theis, P. Gille, P. Ebert, and K. H. Rieder, Phys. Rev. Lett. **89**, 156104 (2002).

[16] H. Takakura, C. P. Gómez, A. Yamamoto, M. de Boissieu, and A. P. Tsai, Nat. Mater. **6**, 58 (2007).

[17] H. R. Sharma, K. Nozawa, J. A. Smerdon, P. J. Nugent, I. McLeod, V. R. Dhanak, M. Shimoda, Y. Ishii, A. P. Tsai, and R. McGrath, Nat. Commun. **4**, 2715 (2013).

[18] S. S. Hars, H. R. Sharma, J. A. Smerdon, S. Coates, K. Nozawa, A. P. Tsai, and R. McGrath, Surf. Sci. **678**, 222 (2018), ISSN 0039-6028.

[19] C. Cui, P. J. Nugent, M. Shimoda, J. Ledieu, V. Fourne, A. P. Tsai, R. McGrath, and H. R. Sharma, Journal of Physics: Condensed Matter **24**, 445011 (2012).